

Recognition of Hg²⁺ Ion through Restricted Imine Isomerization: Crystallographic Evidence and Imaging in Live Cells

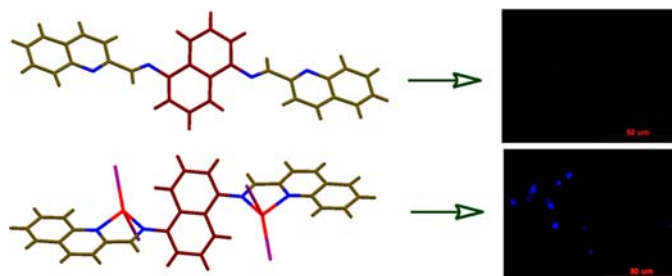
Amal Kumar Mandal,[†] Moorthy Suresh,[†] Priyadip Das,[†] E. Suresh,[†] Mithu Baidya,[‡] Sudip K. Ghosh,^{*,‡} and Amitava Das^{*,†}

Central Salt and Marine Chemicals Research Institute (CSIR), Bhavnagar 364002, Gujarat, India, and Department of Biotechnology, Indian Institute of Technology, Kharagpur, West Bengal 721302, India

amitava@csmcri.org; sudip@hijli.iitkgp.ernet.in

Received April 14, 2012

ABSTRACT



A newly synthesized imine-based receptor (L) showed remarkable specificity toward the Hg²⁺ ion in aqueous media over other metal ions. Coordination of L to Hg²⁺ induces a *turn-on* fluorescence response. This was explained based on the restricted imine isomerization along with PET on coordination to Hg²⁺. X-ray structural evidence tends to favor a C–C bond rotation rather than C=N isomerization for adopting a favorable conformation in L for coordination to Hg²⁺. This reagent could be used for imaging the accumulation of Hg²⁺ ions in HeLa cells.

Mercury is one of the most prevalent toxic metals in the environment and gains access to the body orally or dermally, causing cell dysfunction that consequently leads to health problems.¹ The concern over its deleterious effects on human health has actually led the sensing community to develop new mercury detection methods that are cost-effective, rapid,

facile, and applicable to the environmental and biological milieu.² In this regard, receptor molecules that can provide optical feedback on binding to the Hg²⁺ ion in aqueous or mixed aqueous environments are crucial for developing either colorimetric staining agents³ or fluorescent imaging reagents⁴ for biological applications. Being one of the heavier metal ions, Hg²⁺ generally causes an efficient quenching of the fluorescence through an efficient spin–orbit coupling.⁵ However, any optical feedback that translates the metal ion–receptor binding phenomena into a fluorescence *turn-on* response is preferred over the

[†] Central Salt and Marine Chemicals Research Institute.

[‡] Indian Institute of Technology.

(1) (a) Hutchinson, T. C.; Meena, K. M. In *Lead, Mercury, Cadmium and Arsenic in the Environment*; John Wiley: New York, 1987. (b) Harada, M. *Crit. Rev. Toxicol.* **1995**, *25*, 1–24. (c) Tchounwou, P. B.; Ayensu, W. K.; Ninashvili, N.; Sutton, D. *Environ. Toxicol.* **2003**, *18*, 149–175.

(2) (a) Ros-lis, J. V.; Marcos, M. D.; Martinez-Manez, R.; Rurack, K.; Soto, J. *Angew. Chem., Int. Ed.* **2005**, *44*, 4405–4407. (b) Nolan, E. M.; Lippard, S. J. *Chem. Rev.* **2008**, *108*, 3443–3480.

(3) (a) Brummer, O.; La Clair, J. J.; Janda, K. D. *Org. Lett.* **1999**, *1*, 415–418. (b) Li, T.; Li, B.; Wang, E.; Dong, S. *Chem. Commun.* **2009**, 3551–3553. (c) Aragay, G.; Pons, J.; Merkoçi, A. *Chem. Rev.* **2011**, *111*, 3433–3458. (d) Ma, X.; Wang, J.; Shan, Q.; Tan, Z.; Wei, G.; Wei, D.; Du, Y. *Org. Lett.* **2012**, *14*, 820–823. (e) Saha, S.; Chhatbar, M. U.; Mahato, P.; Praveen, L.; Siddhanta, A. K.; Das, A. *Chem. Commun.* **2012**, *48*, 1659–1661.

(4) (a) Lee, M. H.; Lee, S. W.; Kim, S. H.; Kang, C.; Kim, J. S. *Org. Lett.* **2009**, *11*, 2101–2104. (b) Suresh, M.; Mandal, A. K.; Saha, S.; Suresh, E.; Mandoli, A.; Liddo, R. D.; Parnigotto, P. P.; Das, A. *Org. Lett.* **2010**, *12*, 5406–5409. (c) Dave, N.; Chan, M. Y.; Huang, P. J. J.; Smith, B. D.; Liu, J. J. *Am. Chem. Soc.* **2010**, *132*, 12668–12673. (d) Kumar, M.; Kumar, N.; Bhalla, V.; Singh, H.; Sharma, P. R.; Kaur, T. *Org. Lett.* **2011**, *13*, 1422–1425.

(5) (a) McClure, D. S. *J. Chem. Phys.* **1952**, *20*, 682–686. (b) Masuhara, H.; Shioyama, H.; Saito, T.; Hamada, K.; Yasoshima, S.; Mataga, N. *J. Phys. Chem.* **1984**, *88*, 5868–5873.

fluorescence *turn-off* response for obvious ease in the detection process. Among different signaling mechanisms, photoinduced electron (PET)/energy transfer (PeT),⁶ metal–ligand charge transfer (MLCT),⁷ and intramolecular charge transfer (ICT)⁸ are most common. However, to achieve a reversible *switch-on* fluorescence response on selective binding to Hg²⁺, two common methodologies have been adopted, namely conversion from the nonfluorescent lactam to a strongly fluorescent xanthene form or through achieving a structural rigidity on Hg²⁺ ion binding.⁹ Literature reports are there for demonstrating the second process using azine-based receptors.^{4b} However, such an example using analogous imine isomerization as a signaling mechanism has not been used so far for designing any colorimetric or fluorogenic receptor for Hg²⁺ ion, although it has been documented previously for other metal ions.^{9a}

Herein, we report a novel imine-based molecule (**L**), having naphthalene and quinoline as two photoactive units, for the specific recognition of Hg²⁺ ions through restricted imine isomerization on binding of **L** to Hg²⁺ in mixed aqueous–organic medium. To establish molecular preorganization that takes place prior to the coordination to the Hg²⁺ center, two reference compounds (**L**₁ and **L**₂) were synthesized (Figure 1), and their optical responses on binding to Hg²⁺ were compared with that of **L**. Also, naphthalene (**N**) and quinolone (**Q**) form a FRET pair, and thus, the choice of these two chromophores provides the opportunity to achieve a larger Stokes shift on the sensing event. More importantly, the possibility of using this reagent for imaging application and detection of Hg²⁺ accumulated in cervical cancer cells was explored to check the viability of the cells under the experimental conditions.



Figure 1. Structure of the imine-based receptor molecules.

Reagent **L** and the two reference compounds (**L**₁ and **L**₂) were synthesized following a typical one-step reaction (SI). Various analytical and spectroscopic data agree well with the structure proposed for these reagents and the desired purity. Further, *trans* conformations for three receptors

(6) (a) de Silva, A. P.; Fox, D. B.; Huxley, A. J. M.; Moody, T. *Coord. Chem. Rev.* **2000**, *205*, 41–57. (b) Gunnlaugsson, T.; Davis, A. P.; O'Brien, J. E.; Glynn, M. *Org. Lett.* **2002**, *4*, 2449–2451.

(7) Beer, P. D. *Acc. Chem. Res.* **1998**, *31*, 71.

(8) (a) Xu, Z.; Xiao, Y.; Qian, X.; Cui, J.; Cui, D. *Org. Lett.* **2005**, *7*, 889. (b) Wang, J. B.; Qian, X. F.; Cui, J. N. *J. Org. Chem.* **2006**, *71*, 4308.

(9) (a) Wu, J.; Liu, W.; Ge, J.; Zhang, H.; Wang, P. *Chem. Soc. Rev.* **2011**, *40*, 3483 and the references cited therein. (b) Saha, S.; Mahato, P.; Reddy, U. G.; Suresh, E.; Chakrabarty, A.; Baidya, M.; Ghosh, S. K.; Das, A. *Inorg. Chem.* **2012**, *51*, 336. (c) Mahato, P.; Saha, S.; Suresh, E.; Liddo, R. D.; Parnigotto, P. P.; Conconi, M. T.; Kesharwani, M. K.; Ganguly, B.; Das, A. *Inorg. Chem.* **2012**, *51*, 1769.

were also confirmed from single-crystal X-ray structure analysis.

Spectroscopic properties of **L**, **L**₁, and **L**₂ were investigated in mixed aqueous organic medium (THF/aqueous phosphate buffer (6:4, v/v; pH = 7.2)). The UV–vis spectra of **L** exhibited a strong band at 255 nm ($\epsilon = 58823 \text{ L mol}^{-1} \text{ cm}^{-1}$) with two broad band at 295 nm ($\epsilon = 22768 \text{ L mol}^{-1} \text{ cm}^{-1}$) and 385 nm ($\epsilon = 16096 \text{ L mol}^{-1} \text{ cm}^{-1}$). Electronic spectra of **L** were compared with those of **L**₁ and **L**₂. The bands at ~255 and 295 nm could be attributed to N- and Q-based intracomponent charge-transfer (CT) transitions, respectively, while the broad band at 385 nm was ascribed to a intercomponent CT band with **N** as the donor and **Q** as the acceptor fragment. Addition of a perchlorate salt of alkali, alkaline earth, and common transition-metal ions (Li⁺, Na⁺, K⁺, Cs⁺, Ag⁺, Ca²⁺, Mg²⁺, Sr²⁺, Ba²⁺, Cr³⁺, Fe²⁺, Fe³⁺, Co²⁺, Ni²⁺, Cu²⁺, Zn²⁺, Cd²⁺) did not show any change in electronic spectra of **L**. However, an appreciable change was observed when the spectrum was recorded in the presence of Hg²⁺ (Supporting Information, SI).

Spectral responses of **L**, **L**₁, and **L**₂ on binding to Hg²⁺ in CHCl₃/CH₃CN (1:4 v/v) were different, which were primarily due to the intrinsic difference in the nature of the donor and acceptor fragments in these three receptors. Systematic titration in CHCl₃/CH₃CN (1:4 v/v) medium for **L** revealed the formation of a broader band at longer wavelength (~480 nm). Coordination to Hg²⁺ was expected to favor the intercomponent CT transition and thus the shift to longer wavelength. However, spectral responses for **L** in THF–aqueous phosphate buffer (6:4, v/v; pH = 7.2) were quite different (Figure 2a and inset) and were attributed to a weaker coordination of **L** to hydrated Hg²⁺ ion, as compared to the nonaqueous Hg²⁺ ion in organic medium. Binding affinity of the reagent **L** toward Hg²⁺ in mixed THF–aqueous buffer medium was evaluated by monitoring changes in absorbance at 385 nm (Figure 2b) with varying [Hg²⁺] (0–27 molar equiv).

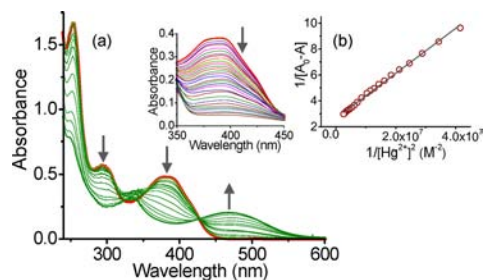


Figure 2. Changes in UV–vis spectra recorded in 25 °C (a) CHCl₃/CH₃CN (1:4 v/v) medium for **L** ($1.8 \times 10^{-5} \text{ M}$) with varying [Hg²⁺] (0 – $1.1 \times 10^{-4} \text{ M}$). Spectra in red indicate **L**. Inset: titration profile for **L** ($2.3 \times 10^{-5} \text{ M}$) with varying [Hg²⁺] (0 – $6.2 \times 10^{-4} \text{ M}$) in THF/aqueous phosphate buffer (6:4, v/v; pH = 7.2) and its corresponding; (b) B–H plot for evaluation of the binding constant for **L** with Hg²⁺. The good fit of the linear plot ($R^2 = 0.99$) confirmed the 2:1 binding stoichiometry.

Weaker binding in aqueous buffer medium was also evident from the much lower affinity constant ($K^A_{[\text{Hg}^{2+}]_2\text{L}} = 1.48 \times 10^7 \text{ M}^{-2} \text{ L}^2$) than the one that was evaluated in $\text{CHCl}_3/\text{CH}_3\text{CN}$ (1:4 v/v) medium ($K^A_{[\text{Hg}^{2+}]_2\text{L}} = 2.79 \times 10^9 \text{ M}^{-2} \text{ L}^2$) under otherwise identical condition. Good linear fit of the Benesi–Hildebrand plot (B–H plot) confirmed the 2:1 binding stoichiometry and formation of $[\text{Hg}^{2+}]_2\text{L}$ complex. This binding stoichiometry in solution was also confirmed from the ESI–mass spectral data (SI). Spectral data also confirmed formation of $[\text{Hg}^{2+}]_2\text{L}_1$ and $[\text{Hg}^{2+}]_2\text{L}_2$ in solution. Further, the single-crystal structure for $[\text{Hg}^{2+}]_2\text{L}$ and $[\text{Hg}^{2+}]_2\text{L}_2$ also corroborated this. No evidence for the stepwise formation of 1:1 and then 2:1 complex could be obtained for **L** and **L**₂, which was evident from the electronic spectral titration profile for **L**₁ (SI). Thus, for reagent **L**, the observed binding constant could be better assigned as the composite binding constant for the formation of $\{\text{L}(\text{Hg}^{2+})_2\}(\text{ClO}_4)_4$.

Emission quantum yields for **L** ($\Phi_{\text{L}} = 0.0011$) and one of the two model receptors ($\Phi_{\text{L}_1} = 0.0118$) were poor. However, relative fluorescence quantum yield for **L**₂ ($\Phi_{\text{L}_2} = 0.1090$) was much higher than that of **L**₁. Because of the flexible nature of the imino compound, the thermal barrier between the two geometrical isomers is low, so the relaxation through photoinduced geometrical change is extremely rapid and efficient.¹⁰ The photoinduced electron transfer (PET) process involving the lone pairs of electrons of $\text{N}_{\text{C}=\text{N}}$ and the excited Q-based fluorophore could also contribute to the observed weaker emission for **L** and **L**₁. Interestingly, the fluorescence enhancement for **L**₂ was only 2-fold on binding to Hg^{2+} ($\Phi^{[\text{Hg}^{2+}]_2\text{L}_2} = 0.2245$), while for similar experiment with **L** ($\Phi^{[\text{Hg}^{2+}]_2\text{L}} = 0.2390$) and **L**₁ ($\Phi^{[\text{Hg}^{2+}]_2\text{L}_1} = 0.2053$) a *switch-on* fluorescence response was observed (Figure 3). This observed enhancement on luminescence response for **L**, **L**₁ and **L**₂ on binding to Hg^{2+} could be ascribed due to the loss of molecular flexibility of these receptors because of restricted imine isomerization. In addition, an interrupted PET process on coordination to the Hg^{2+} was also expected to contribute to this observed *switched-on* emission response.¹¹ It is worth mentioning here that the presence of lower lying CT states (vide supra) could account for the absence of any

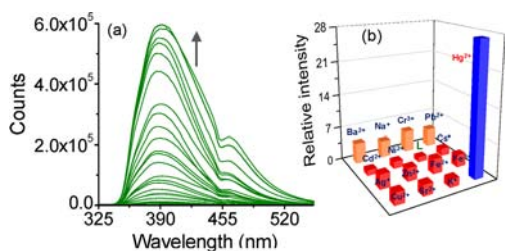


Figure 3. Fluorescence spectral changes in THF–aqueous phosphate buffer medium (6:4, v/v; pH = 7.2) at 25 °C: (a) **L** ($2.0 \times 10^{-5} \text{ M}$) with varying $[\text{Hg}^{2+}]$ (0 – $5.2 \times 10^{-4} \text{ M}$), $\lambda_{\text{exc}} = 295 \text{ nm}$; (b) fluorescence scanning of **L** ($2.0 \times 10^{-5} \text{ M}$) in the presence of various metal ions ($6.0 \times 10^{-4} \text{ M}$) ($\lambda_{\text{exc}} = 295 \text{ nm}$).

N-moiety-based luminescence in **L**, as observed for **L**₂. However, similarities in the luminescence responses of **L** and **L**₁ on binding to Hg^{2+} revealed that the Q-moiety is primarily involved in the photoinduced geometrical isomerization either through rotation about the $\text{C}=\text{N}$ or by $\text{C}_{[\text{Q}]}-\text{N}_{\text{C}=\text{N}}$ bond rotation.

The binding affinity of Hg^{2+} toward **L**, **L**₁, and **L**₂ was evaluated from a Benesi–Hildebrand (B–H) plot using the results of the systematic titrations either by probing the change in fluorescence or absorption band intensity with varying $[\text{Hg}^{2+}]$. Analysis of the B–H plots for **L** and **L**₂ confirmed the 2:1 binding stoichiometry (SI). No spectral evidence for stepwise complex formation was apparent.

However, for **L**₁, two distinct changes in fluorescence spectra were observed when spectra were recorded with varying $[\text{Hg}^{2+}]$ and allowed us to evaluate stepwise binding constants for formation of $[\text{Hg}^{2+}]\text{L}_1$ and $[\text{Hg}^{2+}]_2\text{L}_1$ (SI). The respective binding constants evaluated from different methodologies are summarized in Table 1. The reversible binding of Hg^{2+} to **L** was checked by addition of an aqueous solution of KI (SI). This was also demonstrated by ¹H NMR spectroscopic studies. Because of limited solubility, the ¹H NMR spectra were recorded in a CDCl_3 – $\text{DMSO}-d_6$ (4:1, v/v) medium. On addition of Hg^{2+} , the $\text{H}_{\text{HC}=\text{N}}$ proton showed a drastic downfield shift along with a decrease of signal intensity for the rest of the protons (SI). On addition of excess of thiourea to this solution, the initial spectrum for **L** was restored with a subsequent increase in signal intensity (SI).

Detailed ¹H NMR spectroscopic studies were carried out with an attempt to address the critical issue of bond rotation about the $\text{C}=\text{N}$ or by $\text{C}_{[\text{Q}]}-\text{N}_{\text{C}=\text{N}}$ bond in **L**, **L**₁, and **L**₂ on binding to Hg^{2+} . The 1D-NOE spectra of **L** on selective irradiation of the $\text{H}_{\text{HC}=\text{N}}$ proton at 8.95 ppm showed a correlation at 7.35 ppm, which signified a *trans* orientation of the two N-atoms of Q-ring and $\text{N}_{\text{HC}=\text{N}}$ with respect to each other in solution. No such 1D-NOE correlation was observed in presence of Hg^{2+} (SI). Similar observations were also witnessed for **L**₁ and **L**₂ (SI).

A single-crystal X-ray structure for **L** and **L**₂ revealed that quinolyl and imine nitrogen atoms oriented *trans* to each other (Figure 4a,c), minimizing the proton–proton interactions. Such an orientation is typical for pyridyl-imine ligands.¹² Crystal structures for **L** and $[(\text{Hg})_2\text{L}]_4$ (Figures 4a,b) also revealed change in the twist angle ($\theta_{\text{Q-N}}$)¹³ of 14.6° (42.2° for **L** to 56.8° for $[(\text{Hg})_2\text{L}]_4$) between the terminal Q and central N ring. This change in $\theta_{\text{Q-N}}$ for **L**₂ and $[(\text{Hg})_2\text{L}_2]_4$ was 14.1° (42.2 for **L**₂ to 56.3 for $[(\text{Hg})_2\text{L}_2]_4$) (Figures 4c,d). Thus, structural evidence suggest a difference of $\sim 14^\circ$ in $\theta_{\text{Q-N}}$ to make effective

(10) King, N. R.; Whale, E. A.; Davis, F. J.; Gilbert, A.; Mitchell, G. R. *J. Mater. Chem.* **1997**, *7*, 625–630.

(11) (a) Naik, L. R.; Suresh, H. M.; Inamdar, S. R.; Math, N. N. *Spectrosc. Lett.* **2005**, *38*, 645. (b) Koner, A. L.; Mishra, P. P.; Jha, S.; Dutta, A. *J. Photochem. Photobiol. A.* **2005**, *170*, 21–26.

(12) (a) Kesslen, E. C.; Euler, W. B. *Chem. Mater.* **1999**, *11*, 336–340. (b) Tuna, F.; Hamblin, J.; Clarkson, G.; Errington, W.; Alcock, N. W.; Hannon, M. J. *Chem.—Eur. J.* **2002**, *8*, 4957–4964.

(13) $\theta_{\text{Q-N}}$ is the twist angle between the Q and N rings, while $\theta_{[\text{C}=\text{N}-\text{CNaph}]}$ represents the dihedral angle between planes involving the imine functionality and the naphthalene (N) ring.

Table 1. Association Constants for Complex Formation with Hg^{2+} with Different Receptors in Different Solvent Media^a

K	K_2^{L} (10^5) ($\text{M}^{-2} \text{L}^2$)	$K_1^{\text{L}_1}$ and $K_2^{\text{L}_1 d}$	$K_2^{\text{L}_2}$ (10^5) ($\text{M}^{-2} \text{L}^2$)
abs ^b	148	8700 and $1100 \text{ M}^{-1} \text{L}$	5.84
abs ^c	27900	$1.29 \times 10^9 \text{ M}^{-2} \text{L}^{2e}$	364
fluo ^b	186	10000 and $1500 \text{ M}^{-1} \text{L}$	7.83

^a $K_2^{\text{L}} = K^{[\text{Hg}^{2+}]_2 \text{L}}$; $K_1^{\text{L}_1} = K^{[\text{Hg}^{2+}] \text{L}_1}$; $K_2^{\text{L}_1} = K^{[\text{Hg}^{2+}]_2 \text{L}_1}$; $K_2^{\text{L}_2} = K^{[\text{Hg}^{2+}]_2 \text{L}_2}$. ^b Absorption titration in THF–aqueous phosphate buffer medium (6:4, v/v; pH = 7.2). ^c Signifies absorption titration in $\text{CHCl}_3/\text{CH}_3\text{CN}$ (1:4 v/v) medium. ^d Stepwise (1:1 and then 2:1 with respect to Hg^{2+} and L_1) complex formation was observed for reagent L_1 only in THF–aqueous buffer medium. ^e Composite binding constant was obtained in $\text{CHCl}_3:\text{CH}_3\text{CN}$ (1:4 v/v) medium.

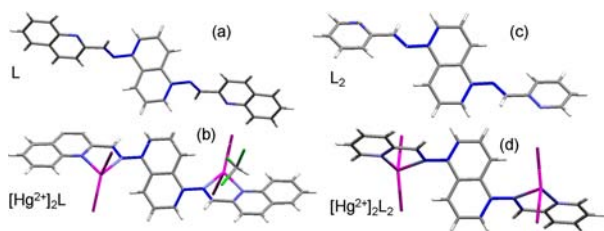


Figure 4. Single crystal structure: (a) L , (b) $[(\text{Hg}_2)\text{L}]_4$, (c) L_2 ; (d) $[(\text{Hg}_2)\text{L}_2]_4$ (solvent molecule was omitted for clarity).

binding to Hg^{2+} either by L or L_2 , while θ involving the N-ring and imine plane ($\theta_{[\text{C}=\text{N}-\text{CNaph}]}$)¹³ was 41.8° and 42.4° for L and L_2 , respectively (SI). Interestingly, a much smaller change in $\theta_{[\text{C}=\text{N}-\text{CNaph}]}$ on binding to the $\text{Hg}(\text{II})$ center was observed ($\theta_{[\text{C}=\text{N}-\text{CNaph}]}$ of 46.01° for $[(\text{Hg}_2)\text{L}]_4$ and 45.1° for $[(\text{Hg}_2)\text{L}_2]_4$), which indicated a nominal perturbation in $\theta_{[\text{C}=\text{N}-\text{CNaph}]}$ upon coordination to the Hg^{2+} center. Thus, structural evidence tends to indicate that $\text{C}_{[\text{O}]}-\text{N}_{\text{C}=\text{N}}$ bond rotation was more plausible than geometrical isomerization around the $\text{C}=\text{N}$.

We explored the possibility of using L and L_1 for the recognition of the Hg^{2+} ion in living cervical cancer cells (HeLa cells) using fluorescence imaging experiments. MTT assay studies revealed that $>80\%$ HeLa cells remained viable even after 12 h of incubation with these probe molecules having concentration comparable to that used for imaging studies (SI). For fluorescence imaging experiments, HeLa cells preexposed to $10 \mu\text{M}$ Hg^{2+} were washed with an appropriate buffer solution and subsequently incubated either with L or with L_1 for 30 min. On viewing through a fluorescence microscope using a 330–380 nm UV filter as an excitation source, a bright blue

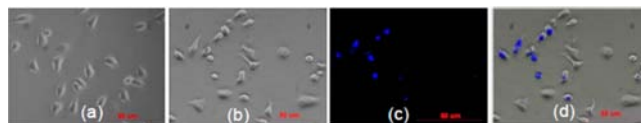


Figure 5. Bright field transmission of living HeLa cells incubated with (a) L ($20 \mu\text{M}$) and (b) L ($20 \mu\text{M}$) with Hg^{2+} ($10 \mu\text{M}$); (c) fluorescence image of HeLa cells incubated with L ($20 \mu\text{M}$) with Hg^{2+} ($10 \mu\text{M}$); (d) merged image of (b) and (c).

fluorescence was observed for HeLa cells pretreated with Hg^{2+} and then with L/L_1 , while no such fluorescence was observed either for untreated HeLa cells or cells treated with only $\text{Hg}(\text{ClO}_4)_2$ (Figure 5).

So, these two probe reagents (L and L_1) were cell membrane permeable and could detect Hg^{2+} uptake in living cells exposed to $[\text{Hg}^{2+}]$ as low as $10 \mu\text{M}$. The reversibility of the binding to L/L_1 and the detection of Hg^{2+} in HeLa cells was established by treating those stained cells with KI ($20 \mu\text{M}$) solution (SI).

In summary, we synthesized an imine-based chemosensor that selectively binds Hg^{2+} ion in aqueous media. We exploited two signal transduction mechanisms, namely, restriction of molecular flexibility and/or PET to achieve fluorescence on response on binding to Hg^{2+} ions. Crystallographic evidence tends to favor the C–C bond rotation, rather than the geometrical isomerization at $\text{C}=\text{N}$ as one of the primary reasons for the restriction of the molecular flexibility on binding to Hg^{2+} . Perhaps for a binucleating receptors like these, cis–trans isomerization is energetically more demanding than the C–C bond rotation. Results of the fluorescence microscopic studies revealed that L and L_1 are cell permeable and could be used as nontoxic imaging reagents for detection of the uptake of Hg^{2+} in the HeLa cells.

Acknowledgment. A.D. thanks DST and CSIR (India) for financial support. A.K.M., M.S., and P.D. acknowledge CSIR for Senior Research Fellowships. M.B. acknowledges UGC (New Delhi) for Jr. Research Fellowship. S.K.G. acknowledges DST for partial grant for the Confocal facility.

Supporting Information Available. Synthetic details, characterization data for the compounds, and selected spectroscopic data. Three crystal structures have been deposited with the Cambridge Crystallographic Data Centre and allocated deposition nos. CCDC 874976–874978. This material is available free of charge via the Internet at <http://pubs.acs.org>.

The authors declare no competing financial interest.